

Thermoelectric response of spin polarization in Rashba spintronic systems

Cong Xiao^{1,2}, Dingping Li^{1,2}, and Zhongshui Ma^{1,2}

¹School of Physics, Peking University, Beijing 100871, China

²Collaborative Innovation Center of Quantum Matter, Beijing, 100871, China

Abstract. Motivated by recent discovery of strongly spin-orbit coupled two-dimensional (2D) electron gas near the surface of Rashba semiconductors BiTeX (X=Cl, Br, I), we calculate thermoelectric responses of spin polarization in 2D Rashba model. By self-consistently determining the energy- and subband-dependent transport time, we present an exact solution of the linearized Boltzmann equation for elastic scattering. Using this solution, we find a non-Edelstein electric-field induced spin polarization which is linear in the Fermi energy E_F , when E_F lies below the band crossing point. The spin polarization efficiency, which is the electric-field induced spin polarization divided by the driven electric current, increases for smaller E_F . It is shown that, as a function of E_F , the temperature-gradient induced spin polarization continuously increases to a saturation value when E_F downs below the band crossing point. As the temperature tends to zero, the temperature-gradient induced spin polarization vanishes.

Keywords: thermoelectric response, Rashba spin-orbit coupling, Boltzmann equation, analytical solution

1. Introduction

Two dimensional (2D) electron systems with spin-orbit coupling (SOC) show a great deal of fascinating transport phenomena due to the mixing of the spin and orbital degrees of freedom, providing the possibility of realizing all-electrical and all-thermal spin control in semiconductor structures. These are the main topics of the rapid developing research fields of spintronics [1] and spin-caloritronics [2]. In the electrical spin control, the generation of a spin current and a nonequilibrium spin polarization transverse to an applied electric field without external magnetic field are remarkable, known as the spin Hall effect [3, 4] and electric-field induced spin polarization [5–7], respectively. Their thermal counterparts toward all-thermal spin control, i.e., the spin Nernst effect [8–12] and temperature-gradient induced spin polarization [13–15], have also attracted more and more interests recently.

The 2D electron system (2DES) with Rashba SOC has been one of the most widely used models to investigate aforementioned effects [8, 10, 13, 14]. In the 2D Rashba model, two bands cross at zero energy, one of them is always positive and the other one

possesses a band valley regime below the band crossing point as shown in Fig. 1. In this valley regime the dispersion curve is not monotonic in momentum space. This regime possesses nontrivial topology of the constant energy surfaces (or Fermi surfaces) [16], which leads to some exciting theoretical predictions, e.g., the enhanced superconducting critical temperature [16], the non-Dyakonov-Perel spin relaxation behavior [17] and the significantly enhanced room-temperature thermoelectric figure of merit [18]. There have been a few theoretical studies [14, 17–20] on the transport properties when the Fermi energy is in or near the band valley regime. However, in Rashba systems formed in conventional narrow-gap semiconductor heterostructures [21], the Rashba spin splitting energy is so small that the band valley structure can not survive the weak disorder broadening and thermal smearing even at very low temperatures. In these systems the Fermi energy usually lies quite above the band crossing point, therefore the band valley is irrelevant to transport.

Recently experimental progress has been made by the discovery of giant bulk and surface Rashba SOC effects in V-VI-VII polar semiconductors BiTeX, (X=Cl, Br, I) [22–24]. In these noncentrosymmetric semiconductors, first-principles calculations and ARPES measurements have clearly demonstrated the existence of 2DES confined near the surface with giant Rashba energy as large as about $10^2 meV$ [25, 26]. In such 2DES, the investigation of electrical and thermal spin control is of significance due to the giant SOC which is promising for spintronics and spin-caloritronics applications. While, when the electron-impurity scattering dominates, for the case that Fermi energies lie below or in the vicinity of the band crossing point, the relaxation time approximation (RTA) used in previous theoretical works on the nonequilibrium spin polarization [14, 20] may not work well due to the giant Rashba SOC. This motivates us to systematically investigate the thermoelectric response of spin polarization in 2DES with giant Rashba SOC, focusing on the consequences of different Fermi surface topologies between the two sides of the band crossing point.

In this paper, we employ the semiclassical Boltzmann equation to calculate the spin polarization induced by electric field and temperature gradient. We focus on the 2D Rashba model at low temperatures where the static impurity scattering dominates. Our calculation is based on an exact transport time solution of the Boltzmann equation in the Born approximation, different from the widely used modified RTA and constant RTA schemes [27]. We show that the electric-field induced spin polarization (EISP) as a function of the Fermi energy E_F behaves differently between the two sides of the band crossing point $E_F = 0$. A linear dependence of EISP on E_F is obtained for $E_F < 0$, differing from the Edelstein result [5] for $E_F \geq 0$. The spin polarization efficiency, defined as the ratio between the EISP and the driven electric-current, increases for lower E_F . The temperature-gradient induced spin polarization (TISP) is calculated, and its dependence on the Fermi energy, changing from large positive values to be quite below the band crossing point, is continuous and monotonic. It is also shown that the temperature-gradient induced spin polarization tends to zero at vanishing temperatures.

2. Semiclassical Boltzmann descriptions of thermoelectric spin responses in Rashba 2DES

2.1. Basic solutions for the 2D Rashba model

We study the 2D Rashba model with spin independent disorder

$$H = \frac{\mathbf{p}^2}{2m} + \frac{\alpha}{\hbar} \boldsymbol{\sigma} \cdot (\mathbf{p} \times \hat{\mathbf{z}}) + V(\mathbf{r}), \quad (1)$$

where $V(\mathbf{r}) = \sum_i V_i \delta(\mathbf{r} - \mathbf{R}_i)$ is the disorder potential produced by randomly distributed δ -scatters at \mathbf{R}_i and is assumed to be standard white-noise disorder: $\langle |V_{\mathbf{k}'\mathbf{k}}|^2 \rangle_{dis} = n_{im} V_0^2$. Here n_{im} is the impurity concentration, $V_{\mathbf{k}'\mathbf{k}}$ the spin-independent part of the disorder matrix element and $\langle \dots \rangle_{dis}$ the disorder average. m is the in-plane effective mass of the conduction electron, $\mathbf{p} = \hbar \mathbf{k}$ the momentum, $\boldsymbol{\sigma} = (\sigma_x, \sigma_y, \sigma_z)$ are the Pauli matrices, α the Rashba coefficient. Eigenenergies of the pure system are $E_{\lambda k} = \frac{\hbar^2 k^2}{2m} + \lambda \alpha k$, with inner eigenstates $|u_{\lambda k}\rangle = \frac{1}{\sqrt{2}} [1, -i\lambda \exp(i\phi)]^T$, where $\lambda = \pm$ and $\tan \phi = k_y/k_x$. The wave number at a given energy $E > 0$ in the λ band is given as $k_\lambda(E) = -\lambda k_R + \frac{1}{\alpha} \sqrt{E_R^2 + 2E_R E}$ (see Fig. 1), where we define the Rashba energy $E_R = m \left(\frac{\alpha}{\hbar}\right)^2$ and $k_R = \frac{E_R}{\alpha}$. The density of state (DOS) at a given $E \geq 0$ is given by $N_{>}(E) = \sum_\lambda N_\lambda(E)$ where

$$N_\lambda(E) = N_0 \frac{k_\lambda(E)}{k_\lambda(E) + \lambda k_R}. \quad (2)$$

Here $N_0 = \frac{m}{2\pi\hbar^2}$ is the DOS of 2D spin polarized parabolic spectrum. For $E > 0$, the group velocity and intraband spin matrix element are given by

$$\mathbf{v}(E, \lambda, \phi) = \frac{N_0}{N_\lambda(E)} \frac{\hbar \mathbf{k}_\lambda(E)}{m} \quad (3)$$

and

$$\langle u_{\lambda \mathbf{k}_\lambda(E)} | \sigma | u_{\lambda \mathbf{k}_\lambda(E)} \rangle = \lambda (\sin \phi \hat{\mathbf{x}} - \cos \phi \hat{\mathbf{y}}), \quad (4)$$

respectively.

The direction of the group velocity is the same as the corresponding momentum due to the isotropic band structure and the monotonic $E - k$ curve when $E \geq 0$. The directions of spin in the two bands at the same polar angle ϕ are opposite to each other.

The lower band has a valley centered at k_R , and the DOS has a one-dimensional (1D) character in the $E_-(k_R) \leq E < 0$ regime [16] with $E_-(k_R) = -\frac{1}{2}E_R$ the energy of the bottom of dispersion curve. For $E_-(k_R) < E < 0$ there are two wave numbers $k_{-2}(E) < k_R < k_{-1}(E)$ with $k_{-\nu}(E) = k_R + (-1)^{\nu-1} \frac{1}{\alpha} \sqrt{E_R^2 + 2E E_R}$, where $-\nu = -1, -2$ denotes the two monotonic branches in this energy regime (see Fig. 1). The DOS $N_{<}(E)$ in the band valley regime is given by $N_{<}(E) = \sum_{\nu=1}^2 N_{-\nu}(E)$ where

$$N_{-\nu}(E) = N_0 \frac{k_{-\nu}(E)}{|k_{-\nu}(E) - k_R|}. \quad (5)$$

For $E_-(k_R) < E < 0$, one obtains

$$\langle u_{-\mathbf{k}_{-\nu}(E)} | \sigma | u_{-\mathbf{k}_{-\nu}(E)} \rangle = -\sin \phi \hat{\mathbf{x}} + \cos \phi \hat{\mathbf{y}} \quad (6)$$

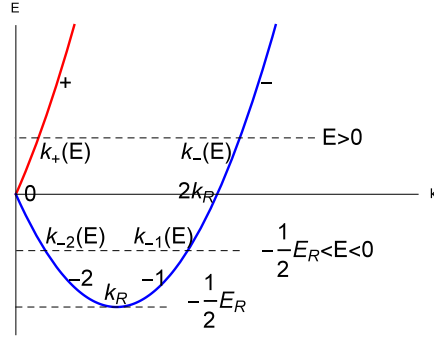


Figure 1. Band structure of the 2D Rashba system. The energy of the band crossing point is chosen to be zero. The wave number and energy of the bottom of the dispersion curve is k_R and $-\frac{1}{2}E_R$, respectively. Corresponding to a given energy $E \geq 0$, the wave number in \pm band is denoted by $k_{\pm}(E)$. For $-\frac{1}{2}E_R < E \leq 0$, there are two monotonic regimes on $E - k$ curve: the one from $k = 0$ to k_R is marked by the branch -2 , whereas the other from $k = k_R$ to $2k_R$ marked by branch -1 . The wave number $k_{-\nu}(E)$ represents the wave number in the $-\nu$ branch at given E , where $\nu = 1, 2$.

and

$$\mathbf{v}(E, -\nu, \phi) = (-1)^{\nu-1} \frac{N_0}{N_{-\nu}(E)} \frac{\hbar \mathbf{k}_{-\nu}(E)}{m}. \quad (7)$$

The direction of the group velocity is parallel (anti-parallel) to the corresponding momentum in $-\nu = -1$ (-2) branch, respectively. This is caused by the non-monotonic $E - k$ curve in the band valley regime. The directions of spin in the two monotonic branches at the same ϕ are the same. These characters show different spin-and group velocity-textures of constant-energy circles between the band valley regime and the $E > 0$ regime.

Exactly at the band crossing point $(E, k) = (0, 0)$, the eigenstate as well as the group velocity and spin matrix element are not well-defined because the polar angle ϕ is arbitrary. However, this does not bring any influence on physical quantities since the DOS at this point is zero, as shown in Eqs. (2) and (5). As for $(E, k) = (0, 2k_R)$, the group velocity and spin matrix element are both well-defined and continuous.

2.2. Basic formulas of nonequilibrium spin polarization and Boltzmann equation

The out-of-equilibrium spin density response to external fields can be obtained in the semiclassical version of linear response theory, which can be decomposed into the intrinsic and extrinsic parts

$$\langle \hat{\sigma} \rangle \equiv \langle \hat{\sigma} \rangle_{int} + \langle \hat{\sigma} \rangle_{ext}, \quad (8)$$

where

$$\begin{aligned} \langle \hat{\sigma} \rangle_{int} &= \sum_l f_l^0 2 \text{Re} \langle \psi_l^{(0)} | \sigma | \delta \psi_l \rangle, \\ \langle \hat{\sigma} \rangle_{ext} &= \sum_l g_l \langle \psi_l^{(0)} | \sigma | \psi_l^{(0)} \rangle. \end{aligned} \quad (9)$$

Here f_l^0 is the equilibrium Fermi-Dirac distribution function (DF) and g_l denotes the out-of-equilibrium change of DF, $l = (\lambda, \mathbf{k})$ is the eigenstate index denoting the band and momentum. $|\psi_l^{(0)}\rangle$ is the eigenstate of the disorder-free Hamiltonian in the absence of external fields, $|\delta\psi_l\rangle$ describes the virtual interband transition induced by the weak external fields.

$\langle\hat{\sigma}\rangle_{int}$ originates from the intrinsic mechanism based solely on the spin-orbit coupled band structure. It is not difficult to verify that $\langle\hat{\sigma}\rangle_{int} = 0$ for the present model, so one only needs to analyze the extrinsic spin density response $\langle\hat{\sigma}\rangle_{ext}$ which depends on the existence of disorder via g_l .

g_l can be calculated by the semiclassical Boltzmann equation in the presence of a uniform weak electric field and small gradients of chemical potential and temperature in nonequilibrium steady states. Here we consider low temperatures where the static impurity scattering dominates the electron relaxation. The Boltzmann equation reads

$$\mathbf{F}_l \cdot \mathbf{v}_l \frac{\partial f_l^0}{\partial E_l} = - \sum_{l'} w_{l',l} [g_l - g_{l'}], \quad (10)$$

where the generalized force acting on the state l is $\mathbf{F}_l = -\frac{E_l - \mu}{T} \nabla T - \nabla \mu + e\mathbf{E}$ with \mathbf{E} , μ , T being the electric field, chemical potential and absolute temperature, respectively. $w_{l',l}$ is the transition rate from state l' to l , which can be determined by the golden rule in the quantum mechanical scattering theory. In the present system without anomalous Hall effect, the lowest order Born approximation is sufficient:

$$w_{l',l} = \frac{1}{\tau_0 N_0} |\langle u_{l'} | u_l \rangle|^2 \delta(E_l - E_{l'}), \quad (11)$$

with $\tau_0 = \left(\frac{2\pi n_{im} V_0^2 N_0}{\hbar} \right)^{-1}$. When $E > 0$, the intraband and interband elastic scattering can be represented by $\omega_{\lambda',\lambda}^{\phi',\phi}(E = E_l) = \int dE_{l'} w_{l',l}$:

$$\omega_{\lambda',\lambda}^{\phi',\phi}(E) = \frac{1}{\tau_0 N_0} \frac{1}{2} [1 + \lambda\lambda' \cos(\phi' - \phi)]. \quad (12)$$

Whereas for $E_-(k_R) < E < 0$ we introduce $\omega_{-\nu',-\nu}^{\phi',\phi}(E = E_l) = \int dE_{l'} w_{l',l}$ to represent the intra-branch and inter-branch scattering:

$$\omega_{-\nu',-\nu}^{\phi',\phi}(E) = \frac{1}{\tau_0 N_0} \frac{1}{2} [1 + \cos(\phi' - \phi)]. \quad (13)$$

3. The exact solution of the Boltzmann equation

In this section we analytically solve the Boltzmann equation based on the isotropic transport times. For $E > 0$, the Boltzmann equation includes both direct intraband and interband elastic scattering; while for $E_-(k_R) < E < 0$, only intraband scattering in the lower band occurs. Due to the band valley structure below the band crossing point, the solution in this regime is nontrivial and completely different from ordinary single-band cases. Finally we clearly show that for positive and negative energies, the DFs are formally similar.

3.1. The exact solution of the Boltzmann equation for $E > 0$

When $E > 0$, the Boltzmann equation can be re-expressed as

$$\begin{aligned} \mathbf{F}_E \cdot \mathbf{v}(E, \lambda, \phi) \partial_E f^0 &= - \sum_{\lambda'} N_{\lambda'}(E) \int \frac{d\phi'}{2\pi} \omega_{\lambda', \lambda}^{\phi', \phi}(E) \\ &\times [g_{\lambda}(E, \vartheta(\mathbf{v}(E, \lambda, \phi))) - g_{\lambda'}(E, \vartheta(\mathbf{v}(E, \lambda', \phi')))], \end{aligned} \quad (14)$$

where $\vartheta(\mathbf{v})$ denotes the angle of the direction of \mathbf{v} with respect to that of the applied generalized force $\mathbf{F}_E = -\frac{E-\mu}{T}\nabla T - \nabla\mu + e\mathbf{E}$. Due to Eq. (3), $\vartheta(\mathbf{v}(E, \lambda, \phi)) = \vartheta(\mathbf{k}_{\lambda}(E))$. Above Boltzmann equation can be solved by introducing the isotropic transport time for electrons with energy E in the λ band as

$$g_{\lambda}(E, \vartheta(\mathbf{k}_{\lambda}(E))) = (-\partial_E f^0) \mathbf{F}_E \cdot \mathbf{v}(E, \lambda, \phi) \tau_{\lambda}(E), \quad (15)$$

and the transport time is determined self-consistently by substituting Eq. (15) into Eq. (14). Thus we obtain

$$\frac{1}{\tau_{\lambda}(E)} = \sum_{\lambda'} N_{\lambda'}(E) \int \frac{d\phi'}{2\pi} \omega_{\lambda', \lambda}^{\phi', \phi}(E) \left[1 - \cos(\phi' - \phi) \frac{\tau_{\lambda'}(E)}{\tau_{\lambda}(E)} \right], \quad (16)$$

where we use the relation $|\mathbf{v}(E, \lambda', \phi')| = |\mathbf{v}(E, \lambda, \phi)|$ suitable for Rashba 2DES. In fact, Eq. (16) contains two coupled linear equations determining τ_+ and τ_- , yields

$$\tau_{\lambda}(E) = \tau_0 \frac{N_{\lambda}(E)}{N_0} \left(\frac{2N_0}{N_{>}(E)} \right)^2. \quad (17)$$

where $N_{>}(E) = 2N_0$. Combining with Eq. (3), the out-of-equilibrium DF takes a compact form

$$g_{\lambda}(E, \vartheta(\mathbf{k}_{\lambda}(E))) = (-\partial_E f^0) \mathbf{F}_E \cdot \frac{\hbar \mathbf{k}_{\lambda}(E)}{m} \tau_0, \quad (18)$$

which satisfies the particle number conservation requirement

$$\sum_{\lambda} \int dE N_{\lambda}(E) \int \frac{d\phi}{2\pi} g_{\lambda}(E, \vartheta(\mathbf{k}_{\lambda}(E))) = 0. \quad (19)$$

Eq. (18) looks similar to the DF for spin degenerate free electron gas without SOC [27], but the important difference is that in the present case the group velocity is given by Eq. (3) rather than $\frac{\hbar \mathbf{k}_{\lambda}(E)}{m}$, for positive energies. This solution is the same as that obtained by employing a custom-designed ansatz for the DF [29] in anisotropic Rashba-Dresselhaus 2DES, while our approach is based on the simple physical picture of isotropic transport time on constant-energy circles. On the other hand, this transport time solution is different from the modified relaxation time approximation (MRTA) solution for isotropic multiband systems: $g_l^{MRTA} = \left(-\frac{\partial f^0}{\partial E_l} \right) \mathbf{F}_l \cdot \mathbf{v}_l \tau_l^{MRTA}$ where

$$\frac{1}{\tau_l^{MRTA}} = \sum_{l'} \omega_{l, l'} \left[1 - \frac{|\mathbf{v}_{l'}|}{|\mathbf{v}_l|} \cos(\vartheta(\mathbf{v}_l) - \vartheta(\mathbf{v}_{l'})) \right]. \quad (20)$$

Comparing Eq. (20) with (16), it is obvious that this MRTA solution can not be self-consistently obtained from the Boltzmann equation for Rashba 2DEG, because if

one substitutes above g_l^{MRTA} into the Boltzmann equation, it is Eq. (16) rather than Eq. (20) that will be arrived at for τ_l^{MRTA} . Thus the MRTA only makes sense as an approximate solution for Rashba 2DES. We can further point out that, in the present model, the result of Eq. (20) is the same as Eq. (17) only in the zeroth order of SOC while different from the latter even in the 1st order of SOC in the small SOC limit. Thus this MRTA in Rashba 2DEG even can not be regarded as a better one than the constant RTA obtained by neglecting the scattering-in term directly.

3.2. The exact solution of the Boltzmann equation for $E_-(k_R) < E < 0$

When $E_-(k_R) < E < 0$, by converting the momentum integration in Eq. (10) into energy integration and noticing the different orientations of group velocity in the two monotonic branches, the Boltzmann equation can be re-expressed as

$$\begin{aligned} \mathbf{F}_E \cdot \mathbf{v}(E, -\nu, \phi) \partial_E f^0 &= - \sum_{\nu'} N_{-\nu'}(E) \int \frac{d\phi'}{2\pi} \omega_{-\nu', -\nu}^{\phi', \phi}(E) \\ &\times [g_{-\nu}(E, \vartheta(\mathbf{v}(E, -\nu, \phi))) - g_{-\nu'}(E, \vartheta(\mathbf{v}(E, -\nu', \phi')))], \end{aligned} \quad (21)$$

which is similar to Eq. (14) for $E > 0$. The derivation of the transport time solution of Eq. (21) is thus similar to that when $E > 0$. Substituting

$$g_{-\nu}(E, \vartheta(\mathbf{v}(E, -\nu, \phi))) = (-\partial_E f^0) \mathbf{F}_E \cdot \mathbf{v}(E, -\nu, \phi) \tau_{-\nu}(E) \quad (22)$$

into Eq. (21), taking into account the fact that in the band valley regime the direction of the group velocity can be parallel or anti-parallel to that of the momentum, i.e., $\vartheta(\mathbf{v}(E, -1, \phi)) = \vartheta(\mathbf{k}_{-1}(E))$, $\vartheta(\mathbf{v}(E, -2, \phi)) = \vartheta(\mathbf{k}_{-2}(E)) + \pi$ and then

$$\frac{\cos \vartheta(\mathbf{v}(E, -\nu', \phi'))}{\cos \vartheta(\mathbf{v}(E, -\nu, \phi))} = (-1)^{\nu' - \nu} \frac{\cos \vartheta(\mathbf{k}_{-\nu'}(E))}{\cos \vartheta(\mathbf{k}_{-\nu}(E))}, \quad (23)$$

we get the following self-consistent equation for $\tau_{-\nu}$:

$$\begin{aligned} \frac{1}{\tau_{-\nu}(E)} &= \sum_{\nu'} N_{-\nu'}(E) \int \frac{d\phi'}{2\pi} \omega_{-\nu', -\nu}^{\phi', \phi}(E) \\ &\times \left[1 - (-1)^{\nu' - \nu} \cos(\phi' - \phi) \frac{\tau_{-\nu'}(E)}{\tau_{-\nu}(E)} \right]. \end{aligned} \quad (24)$$

Here we have used the relation $|\mathbf{v}(E, -\nu', \phi')| = |\mathbf{v}(E, -\nu, \phi)|$. Then the transport time is found as

$$\tau_{-\nu}(E) = \tau_0 \frac{N_{-\nu}(E)}{N_0} \left(\frac{2N_0}{N_{<}(E)} \right)^2. \quad (25)$$

where $\left(\frac{2N_0}{N_{<}(E)} \right)^2 = \frac{E_R^2 + 2E_R E}{E_R^2}$. Comparing this transport time for negative energies to Eq. (17) for positive energies, one can see that they share the same form.

Therefore the nonequilibrium DF satisfying the particle number conservation requirement is

$$g_{-\nu}(E) = (-\partial_E f^0) \mathbf{F}_E \cdot \left[(-1)^{\nu-1} \frac{\hbar \mathbf{k}_{-\nu}(E)}{m} \right] \tau_0 \left(\frac{2N_0}{N_{<}(E)} \right)^2. \quad (26)$$

Here and below we use the simplified notation $g_\lambda(E)$ and $g_{-\nu}(E)$ to represent the DF for brevity. It is obvious that this DF for negative energies is formally similar to that for positive energies when the latter is re-expressed as

$$g_\lambda(E) = (-\partial_E f^0) \mathbf{F}_E \cdot \frac{\hbar \mathbf{k}_\lambda(E)}{m} \tau_0 \left(\frac{2N_0}{N_>(E)} \right)^2, \quad (27)$$

except one significant difference: the $(-1)^{\nu-1}$ factor for negative energies. This factor denotes nothing but the important fact that, for electrons with negative energy on the branch $\nu = 2$, the group velocity and momentum has the opposite directions (see Eq. (7) and Fig.1).

By Eqs. (18) and (26), the out-of-equilibrium DFs in above two energy regimes are continuous at $E = 0$: $g_+(E \rightarrow 0^+) = g_{-2}(E \rightarrow 0^-) = 0$, $g_{-1}(E \rightarrow 0^-) = g_-(E \rightarrow 0^+)$.

4. Electric-field and temperature-gradient induced spin polarization

Since the nonequilibrium state is driven by the effective electric field $\mathbf{E}^* = \mathbf{E} - \frac{1}{e} \nabla \mu$ and temperature gradient $(-\nabla T)$, the spin density response takes the following form in the linear response regime

$$\langle \hat{\sigma} \rangle_{ext} = \chi_{\mathbf{E}} \cdot \mathbf{E}^* + \chi_{\nabla T} \cdot (-\nabla T). \quad (28)$$

Here the EISP coefficient $\chi_{\mathbf{E}}$ and TISP coefficient $\chi_{\nabla T}$ can be calculated from the 2nd equation of Eq. (9), where the momentum integration is performed by integrating over energy and polar angle. Substituting the out of equilibrium DF, i.e., Eqs. (18) and (26), the $\chi_{\mathbf{E}}$ and $\chi_{\nabla T}$ containing contributions from both bands are given by $\chi_{\mathbf{E}}(T, \mu) = \chi_{\mathbf{E},+}(T, \mu) + \chi_{\mathbf{E},-}(T, \mu)$:

$$\begin{aligned} \chi_{\mathbf{E},+}(T, \mu) &= e \int \frac{d\phi}{2\pi} \int_0^\infty dE N_+(E) (-\partial_E f^0) \mathbf{v}(E, +, \phi) \\ &\times \tau_+(E) \langle u_{\mathbf{k}_+(E)} | \sigma | u_{\mathbf{k}_+(E)} \rangle, \\ \chi_{\mathbf{E},-}(T, \mu) &= e \int \frac{d\phi}{2\pi} \int_0^\infty dE N_-(E) (-\partial_E f^0) \mathbf{v}(E, -, \phi) \\ &\times \tau_-(E) \langle u_{\mathbf{k}_-(E)} | \sigma | u_{\mathbf{k}_-(E)} \rangle \\ &+ e \int \frac{d\phi}{2\pi} \int_{E_-(k_R)}^0 dE \sum_\nu N_{-\nu}(E) (-\partial_E f^0) \\ &\times \mathbf{v}(E, -\nu, \phi) \tau_{-\nu}(E) \langle u_{\mathbf{k}_{-\nu}(E)} | \sigma | u_{\mathbf{k}_{-\nu}(E)} \rangle, \end{aligned} \quad (29)$$

and

$$\chi_{\nabla T}(T, \mu) = \frac{1}{e} \int_{E_-(k_R)}^\infty dE (-\partial_E f^0) \frac{E - \mu}{T} \chi_{\mathbf{E}}(E). \quad (30)$$

Here and below we use the simplified notation $\chi_{\mathbf{E}}(E)$ to represent the zero-temperature EISP coefficient $\chi_{\mathbf{E}}(T = 0, E)$ for brevity. $\chi_{\mathbf{E}}$ is a tensor and has two indices: $\chi_{\mathbf{E}}(i, j)$ where i specifies the spin component, and j the direction of the electric field. Due to the isotropy, we can apply the generalized force only in x direction for the calculation, and only $\chi_{\mathbf{E}}(\hat{y}, \hat{x})$ will be calculated below ($\chi_{\mathbf{E}}(\hat{x}, \hat{x}) = 0$). Also we will drop the indices (\hat{y}, \hat{x}) in $\chi_{\mathbf{E}}(\hat{y}, \hat{x})$, for simplicity, $\chi_{\mathbf{E}}$.

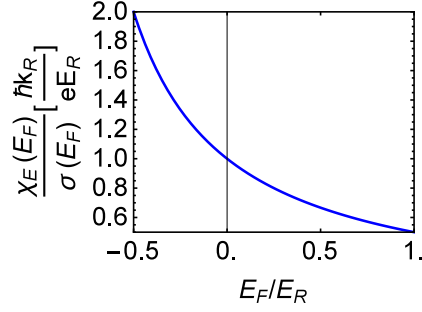


Figure 2. Spin polarization efficiency.

4.1. EISP

The zero-temperature EISP for $E_F \geq 0$ can be obtained easily from Eq. (29) as

$$\chi_{\mathbf{E}}(E_F \geq 0) = e\tau_0 \frac{\alpha}{\hbar} 2N_0. \quad (31)$$

This result has been well-known since Edelstein [5]. It is independent on the Fermi energy, because the directions of spin on the inner (+) and outer (−) Fermi circles are opposite at the same polar angle ϕ and the E_F -dependence of EISPs in both Fermi circles cancels.

While, for Fermi energies below the band crossing point, the EISP takes the following non-Edelstein form

$$\chi_{\mathbf{E}}(E_F \leq 0) = e\tau_0 \frac{\alpha}{\hbar} 2N_0 \left(1 + \frac{2E_F}{E_R} \right). \quad (32)$$

It is linearly dependent on the Fermi energy, different from the positive Fermi energy case. In the band valley, the orientations of spin on the inner (−2) and outer (−1) Fermi circles are parallel at the same ϕ and the E_F -dependence of EISPs of both Fermi circles does not cancel. Since the Fermi surface topology in the band valley differs from that above the band crossing point, the behaviors of EISPs are different between the two regimes. $\chi_{\mathbf{E}}(E)$ is continuous at $E = 0$. The contribution to $\chi_{\mathbf{E}}(0)$ entirely comes from the outer Fermi circle ($E_F = 0, k = 2k_R$), since the DOS at the band crossing point ($E_F = 0, k = 0$) is zero.

We compare Eqs. (31) and (32) to the EISP obtained by employing the constant RTA [14]: $\chi_{\mathbf{E}}^{RTA}(E_F \geq 0) = e\tau \frac{\alpha}{\hbar} 2N_0$, $\chi_{\mathbf{E}}^{RTA}(E_F \leq 0) = e\tau \frac{\alpha}{\hbar} 2N_0 \sqrt{1 + \frac{2E_F}{E_R}}$, with τ the constant relaxation time independent on the energy and band. For $E_F \geq 0$ the EISP obtained by the constant RTA has the same Edelstein form, while when $E_F \leq 0$ the constant RTA result shows different E_F -dependence from Eq. (32).

Now we calculate the spin polarization efficiency, defined as the ratio between the electrical-field induced spin polarization and the driven electric-current density. The electrical conductivity for the same model has been given by [28]: $\sigma(E_F \geq 0) = \frac{e^2}{2\pi^2\hbar} \frac{2\pi(E_F+E_R)\tau_0}{\hbar}$, $\sigma(E_F \leq 0) = \frac{e^2}{2\pi^2\hbar} \frac{2\pi(E_F+E_R)\tau_0}{\hbar} \left(1 + \frac{2E_F}{E_R} \right)$. Therefore, the spin polarization efficiency is given by a single expression suitable for both positive and

negative Fermi energies

$$\frac{\chi_{\mathbf{E}}(E_F)}{\sigma(E_F)} = \frac{\hbar k_R}{e E_R} \frac{1}{1 + \frac{E_F}{E_R}}, \quad (33)$$

which increases for decreased Fermi energies (shown in Fig. 2). Eqs. (31), (32) and (33) show that when the Fermi energy lies below the band crossing point, although the EISP is lowered, higher spin polarization efficiency is achieved.

4.2. TISP

We substitute $\chi_{\mathbf{E}}(E)$ into Eq. (30), and define

$$\begin{aligned} \frac{E - \mu}{k_B T} &= x, \quad \frac{\mu}{k_B T} = -t_1, \quad \frac{E_F}{k_B T} = -t_2, \\ a(t_1) &= \int_{t_1}^{\infty} dx \left(-\frac{\partial f^0}{\partial x} \right) x, \quad b(t_1) = \int_{t_1}^{\infty} dx \left(-\frac{\partial f^0}{\partial x} \right) x^2, \end{aligned} \quad (34)$$

then the TISP is found as

$$\chi_{\nabla T} = \frac{k_B}{e} \chi_{\mathbf{E}}(0) \frac{2k_B T}{E_R} \frac{\pi^2}{3} \left[1 - \frac{b(t_1) - t_1 a(t_1)}{\pi^2/3} \right]. \quad (35)$$

The relation between t_2 and t_1 (i.e., the chemical potential at low temperatures) can be obtained by the consideration about electron density [27]

$$\begin{aligned} t_2 - t_1 &= 0, \quad E_F \gg k_B T, \\ t_2 - t_1 &= o\left(\frac{k_B T}{E_R}\right), \quad |E_F| \sim k_B T, \\ t_2 - t_1 &= \frac{\pi^2}{6} \frac{k_B T}{E_R + 2E_F}, \quad -E_F \gg k_B T. \end{aligned} \quad (36)$$

Here we only consider small thermal fluctuations $k_B T \ll E_R$ and $E_F + \frac{1}{2}E_R \gg k_B T$, so that the band valley structure and the Fermi surfaces survive the thermal smearing. In some new materials with giant Rashba effect, e.g., strongly spin-orbit coupled 2DES near the surface of Rashba semiconductors BiTeX (X=Cl, Br, I), E_R is about $35 \sim 200 meV$. Therefore, $k_B T \ll E_R$ and $E_F + \frac{1}{2}E_R \gg k_B T$ can be satisfied at low temperatures about several Kelvins for not too low Fermi energies.

Consequently we can set $t_2 = t_1$ in the expression for $\chi_{\nabla T}$ since Eq. (35) has already been $o\left(\frac{k_B T}{E_R}\right)$:

$$\chi_{\nabla T} = \tau_0 \frac{\alpha}{\hbar} 2N_0 k_B \frac{\pi^2}{3} \left[1 - 3 \frac{b(t_1) - t_1 a(t_1)}{\pi^2} \right] \frac{2k_B T}{E_R}. \quad (37)$$

This is our main analytical result for TISP. This formula is still valid for Fermi energies near the band crossing point, where the Sommerfeld expansion is not suitable for the treatment of Eq. (30), due to the fact that the energy-derivative of $\chi_{\mathbf{E}}(E)$ is not continuous at the band crossing point.

According to Eq. (37), $\chi_{\nabla T}$ is given in Fig. 3, in units of $\tau_0 \frac{\alpha}{\hbar} 2N_0 k_B \frac{\pi^2}{3} \frac{2k_B T}{E_R}$. When $E_F/k_B T \gtrsim 5$, $\chi_{\nabla T}$ almost vanishes. When $E_F/k_B T \lesssim -5$, $\chi_{\nabla T}/\tau_0 \frac{\alpha}{\hbar} 2N_0 k_B \frac{\pi^2}{3} \frac{2k_B T}{E_R}$

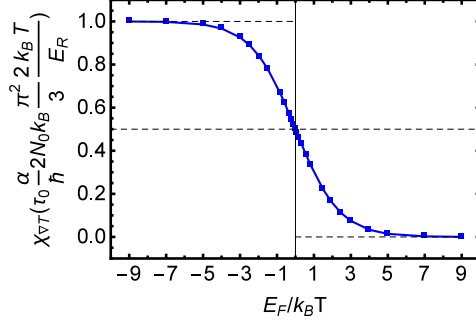


Figure 3. Temperature-gradient induced spin polarization.

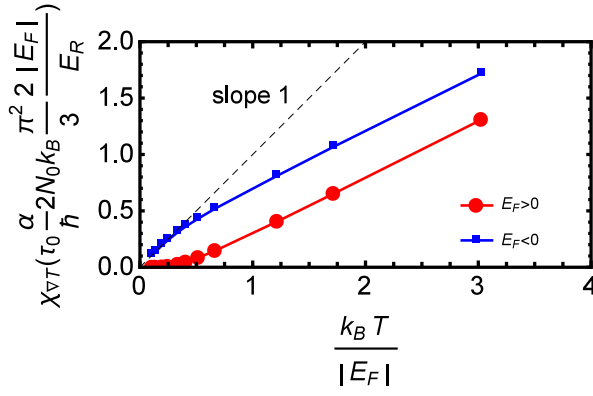


Figure 4. The Temperature dependence of $\chi_{\nabla T}$ for positive Fermi energy (red curve) and negative Fermi energy (blue curve).

approaches a constant value 1. In the intermediate regime $-5 \lesssim E_F/k_B T \lesssim 5$, $\chi_{\nabla T}$ is monotonically decreasing as $E_F/k_B T$ increases.

Eq. (37) can be re-arranged as

$$\chi_{\nabla T} = \tau_0 \frac{\alpha}{\hbar} 2N_0 k_B \frac{\pi^2}{3} \frac{2|E_F|}{E_R} \left[1 - \frac{b(t_2) - t_2 a(t_2)}{\pi^2/3} \right] \frac{1}{|-t_2|}. \quad (38)$$

To make the temperature dependence of $\chi_{\nabla T}$ clear, we replot $\chi_{\nabla T}$ (in units of $\tau_0 \frac{\alpha}{\hbar} 2N_0 k_B \frac{\pi^2}{3} \frac{2|E_F|}{E_R}$) as function of $\frac{k_B T}{|E_F|}$ ($\frac{1}{|-t_2|}$) in Fig. 4.

It shows that $\chi_{\nabla T}$ increases with increasing temperature. When $k_B T/E_F \lesssim 0.2$, $\chi_{\nabla T}$ fully vanishes, when $k_B T/E_F$ continues to increase the contribution of the band valley structure will be included and dominates $\chi_{\nabla T}$, then $\chi_{\nabla T}$ is enhanced. When $k_B T/(-E_F) \lesssim 0.2$, $\chi_{\nabla T}/\tau_0 \frac{\alpha}{\hbar} 2N_0 k_B \frac{\pi^2}{3} \frac{2(-E_F)}{E_R}$ is almost exactly linear in $k_B T/(-E_F)$ with slope 1. When the temperature increases, not only the band valley contributes, but also the electron states above the band crossing point are included due to the thermal smearing, thus the TISP is suppressed. Moreover, when $\frac{k_B T}{|E_F|} \gg 1$, $t_2 \rightarrow 0$, $1 - 3 \frac{b(t_2) - t_2 a(t_2)}{\pi^2} \rightarrow \frac{1}{2}$, so $\chi_{\nabla T} \left(\frac{k_B T}{|E_F|} \gg 1 \right) \rightarrow \chi_{\nabla T}(E_F = 0) = \tau_0 \frac{\alpha}{\hbar} 2N_0 k_B \frac{\pi^2}{3} \frac{1}{2} \frac{2k_B T}{E_R}$ linear in T .

5. Conclusions

In conclusion, we have calculated the thermoelectric responses of spin polarization in 2D Rashba system. By self-consistently determining the transport time, we exactly solved the Boltzmann equation when static impurity scatterings dominate the electron relaxation process. It was shown that the electric-field induced spin polarization is linearly dependent on the Fermi energy when only the lower band is occupied, different from the Edelstein behavior when both bands occupied. Higher spin polarization efficiency is achieved when the Fermi energy lies below the band crossing point. It was found that the temperature-gradient induced spin polarization continuously increase to a saturation value as the Fermi energy decreases below the band crossing point. In addition, the temperature-gradient induced spin polarization tends to zero at vanishing temperatures.

This work may stimulate more experimental and theoretical works on the electrical and thermal spin control in Rashba semiconductors BiTeX ($X=\text{Cl, Br, I}$) and BiTeX quantum wells, as well as other materials with giant Rashba spin splitting.

Acknowledgments

The Work is supported by National Natural Science Foundation of China (No. 11274013 and No. 11274018), and Ministry of Science and Technology of the People's Republic of China (2012CB921300).

References

- [1] Zutic I, Fabian J, and Sarma S D 2004 Rev. Mod. Phys. **76**, 323
- [2] Bauer G E W, Saitoh E, and van Wees B J 2012 Nat. Mater. **11**, 391
- [3] Sinova J, Culcer D, Niu Q, Sinitsyn N A, Jungwirth T, and MacDonald A H 2004 Phys. Rev. Lett. **92**, 126603
- [4] Hirsch J E 1999 Phys. Rev. Lett. **83**, 1834
- [5] Edelstein V M 1990 Sol. State Communs. **73**, 233
- [6] Mishchenko E G, Shytov A V, and Halperin B I 2004 Phys. Rev. Lett. **93**, 226602
- [7] Gorini C, Schwab P, Dzierzawa M, and Raimondi R 2008 Phys. Rev. B **78**, 125327
- [8] Ma Z 2010 Solid State Commun. **150**, 510
- [9] Akera H and Suzuura H 2013 Phys. Rev. B **87**, 075301
- [10] Borge J, Gorini C, and Raimondi R 2013 Phys. Rev. B **87**, 085309
- [11] Iglesias P E and Maytorena J A 2014 Phys. Rev. B **89**, 155432
- [12] Tauber K, Gradhand M, Fedorov D V, and Mertig I 2012 Phys. Rev. Lett. **109**, 026601
- [13] Wang C M and Pang M Q 2010 Solid State Commun. **150**, 1509
- [14] Dyrdal A, Ingot M, Dugaev V K, and Barnas J 2013 Phys. Rev. B **87**, 245309
- [15] Tolle S and Gorini C, and Eckern U 2014 Phys. Rev. B **90**, 235117
- [16] Cappelluti E, Grimaldi C, and Marsiglio F 2007 Phys. Rev. Lett. **98**, 167002
- [17] Grimaldi C 2005 Phys. Rev. B **72**, 075307
- [18] Wu L, Yang J, Wang S, Wei P, Yang J, Zhang W, and Chen L 2014 Appl. Phys. Lett. **105**, 202115
- [19] Grimaldi C, Cappelluti E, and Marsiglio F 2006 Phys. Rev. B **73**, 081303(R)
- [20] Tsutsui K and Murakami S 2012 Phys. Rev. B **86**, 115201

- [21] Nitta J, Akazaki T, Takayanagi H, and Enoki T 1997 Phys. Rev. Lett. **78**, 1335
- [22] Ereemeev S V, Nechaev I A, Koroteev Yu M, Echenique P M, and Chulkov E V 2012 Phys. Rev. Lett. **108**, 246802; Ereemeev S V, Rusinov I P, Nechaev I A, and Chulkov E V 2013 New J. Phys. **15**, 075015
- [23] Landolt G et al. 2012 Phys. Rev. Lett. **109**, 116403; Landolt G et al. 2013 New. J. Phys. **15**, 085022
- [24] Crepaldi A et al. 2012 Phys. Rev. Lett. **109**, 096803
- [25] Sakano M et al. 2013 Phys. Rev. Lett. **110**, 107204
- [26] Rusinov I P, Nechaev I A, Ereemeev S V, Friedrich C, Blugel S, and Chulkov E V 2013 Phys. Rev. B **87**, 205103
- [27] Ziman J M 1972 Principles of the Theory of Solids (Cambridge University Press, Cambridge)
- [28] Xiao C, Li D P, and Ma Z S arXiv:1507.04237
- [29] Trushin M and Schliemann J 2007 Phys. Rev. B **75**, 155323